International Journal of Applied Earth Observations and Geoinformation 95 (2021) 102243

Contents lists available at ScienceDirect

International Journal of Applied Earth Observations and Geoinformation

journal homepage: www.elsevier.com/locate/jag

A methodology to estimate forest fires burned areas and burn severity degrees using Sentinel-2 data. Application to the October 2017 fires in the Iberian Peninsula

Rafael Llorens [a], José Antonio Sobrino [a,*], Cristina Fernández [b], José M. Fernández-Alonso [b], José Antonio Vega [b]

[a] Global Change Unit, Image Processing Laboratory, University of Valencia, Paterna, E-46980, Spain
[b] Centro de Investigación Forestal de Lourizán, Xunta de Galicia, Pontevedra, E-36156, Spain

ARTICLE INFO

Keywords:
Wildfires
EFFIS
Sentinel-2
dNBR
Fire perimeter
Burn severity levels

ABSTRACT

A methodology to estimate the extent of areas affected by forest fires, as well as the burn severity levels using Sentinel 2 images (10 and 20 m) is proposed and applied to the fires occurred in October 2017 in Spain and Portugal. An extension larger than 250,000 ha and 4 burn severity levels (low, moderate, high and very high) have been obtained. The comparison with the European Forest Fire Information System (EFFIS), which uses MODIS images (250 m), shows that the methodology improves the area estimate by 10 % in commission area. In terms of burn severity levels, the Separability index (SI) and the Kappa statistic (k) show a high correlation between Sentinel-2 and EFFIS (SI values higher than one in all cases and k higher than 0.69, respectively).

1. Introduction

Forest fires, together with climate change and drought, are considered one of the main disturbances, which cause, among other impacts, the destruction of vegetation in the Iberian Peninsula (Sousa, 1984). Climate change entails a major challenge for forests, particularly for Mediterranean areas, where the probability of extreme events is expected to increase (Lindner et al., 2010). In recent years, the temperatures increasing and the precipitation decreasing have led to an increase in fires hazard (Vilar et al., 2016) and, therefore, a higher emission of gases (CO_2, CO, and CH_4) related to the greenhouse effect (Seiler and Crutzen, 1980; Bergamaschi et al., 2000). As a result of the high severity level achieved in some fires, human life, infrastructures and ecosystem services have been put at risk (Vega et al., 2013). However, there are cases where forest fires help the ecosystem such as crop fields (once harvested) are usually burned in order to fertilize the soil and eliminate the bad weed before sowing (Vélez et al., 1990).

Nowadays, remote sensing is a key tool for the monitoring, analysis and restoration of burned areas on a global and regional scale, because it provides reliable and quick results and allows rapid diagnosis over burned areas for post-fire mitigation activities (Chuvieco et al., 2003; Chuvieco, 2009; Sobrino et al., 2019). In this sense, the multispectral instrument (MSI) aboard the satellite constellation Sentinel-2 offers the possibility of obtaining information in medium and high spatial resolution (10–20 m) (ESA, 2015; Van der Meer et al., 2014; Van der Werff and Van der Meer, 2015). In addition, the MSI sensor provides spectral information in different bands, being the near infrared (NIR) and the short wave infrared (SWIR) the regions where there is the highest difference between burned and unburned area (Fernández-Manso et al., 2016; Escuin et al., 2008). Recent studies, using Sentinel-2 spectral indices, show a high correlation with burned areas and burn severity levels within burned areas measured in fieldworks (Fernández-Manso et al., 2016; Lutes et al., 2006; Mallinis et al., 2018; Huang et al., 2016). The most commonly used index is the differenced Normalized Burn Ratio (dNBR) with bands in the NIR and SWIR regions (Fernández-Manso et al., 2016). This index considers the NIR and SWIR spectral regions because they are less sensitive to atmospheric effects, and can accurate quantify the vegetation affected and the reduction of canopy moisture (a decrease in NIR regions and increase in SWIR region in the post-fire scenario) (Teodoro and Amaral, 2019; Amos et al., 2019). Therefore, the higher reflectance difference (higher than 0) between NIR and SWIR regions, the higher fire burn severity degree. The dNBR index

* Corresponding author.
E-mail addresses: rafael.llorens@uv.es (R. Llorens), sobrino@uv.es (J.A. Sobrino), cristina.fernandez.filgueira@xunta.es (C. Fernández), josemfernandez@uvigo.es (J.M. Fernández-Alonso), jalvh@hotmail.es (J.A. Vega).

https://doi.org/10.1016/j.jag.2020.102243
Received 15 January 2020; Received in revised form 14 September 2020; Accepted 21 September 2020
Available online 11 October 2020

can also provide information on vegetation regeneration. Once vegetation regeneration has begun, the fire scar will begin to reflect a stronger signal in the NIR region of the spectrum because healthy plants reflect strongly in the NIR portion due to the properties of chlorophyll. Therefore, negative values of dNBR indicate regeneration of vegetation. It is also necessary to take into account the time elapsed between the fire occurrence and the images acquisition in order to be able to verify which moment is better suited to reality. For this reason, pre and post-fire images should be chosen as close to the fire date as possible or it could negatively impact their dNBR values. Multitemporal remote sensing data can provide information before, during and after a wildfire, which can improve the surface characteristic changes detection of burnt areas including fuel consumption, soil color alteration and vegetation recovery (White et al., 1996; Chen et al., 2011).

In addition to Sentinel-2 burned area detection and burn severity levels, the Copernicus program is the main source of European wildfires information. Specifically, the European Forest Fire Information Service (EFFIS), which is a meteorological and satellite mapping system database developed by the Joint Research Centre (JRC) and the Copernicus Emergency Mapping Service (EMS), with worldwide coverage, addresses a wide range of emergencies resulting from disasters (Giglio et al., 2003; Roy et al., 2005, 2007; Neumann et al., 2007; Twele, 2004; Navarro et al., 2017).

To validate burned area results, MAPAMA (Ministerio de Agricultura, Pesca y Alimentación), ICNF (Instituto para a Conservação da Natureza e das Florestas), and EMS (Emergency Mapping Service) maps are used as references. In burn severity levels sense, the EFFIS data is used because is the only reference information at global level. These burned areas reference data are based on GPS measurements, regional cartography and remote sensing data and the EFFIS data is based on

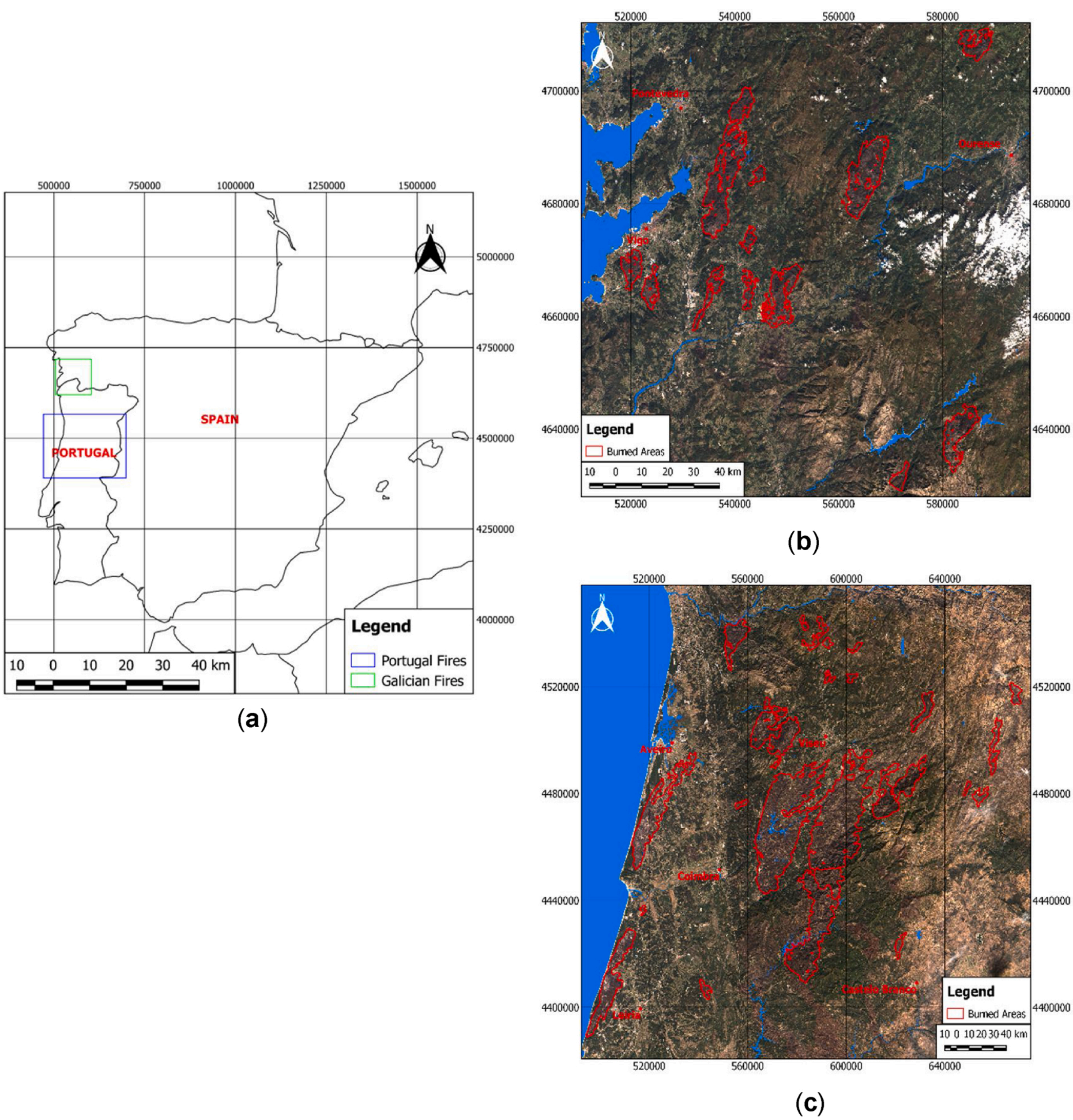

Fig. 1. **(a)** Wildfires study region located in northwestern Spain (color green) and in Portugal (color blue). **(b)** Focus map of Galicia wildfires region with burned areas perimeters (red color). **(c)** Focus map of Portugal wildfires region with burned areas perimeters (red color). The reference coordinate system is WGS 84 / UTM zone 29 N (EPSG: 32,629) and the water areas are masked (blue color). (For interpretation of the references to colour in the Figure, the reader is referred to the web version of this article).

dNBR algorithm using the Moderate Resolution Imaging Spectroradiometer (MODIS) sensor.

The aim of this article is to demonstrate the use of Sentinel-2 dNBR index as a good alternative to EFFIS estimate to delimit fire perimeters (quantifying burned areas) and asses the burn severity levels in the vegetation strata within burned areas in Iberian Peninsula (Spain and Portugal) in October 2017.

2. Materials and methods

2.1. Study area

The wildfires events exposed in this article occurred in Galicia (northwestern Spain) and in Portugal during the autumn of 2017, (all of them bigger than 500 ha). Those fires burned more than 250,000 ha from 2 to 16 October (Fig. 1), aff ;ecting both forest and wildland–urban interface areas. According to the 2012 Corine Land Cover (CLC2012), the study fires aff ;ected mainly broad-leaved forest (25 %), coniferous forest (15 %), mixed forest (10 %), shrubland (30 %) and transitional woodland-shrub (20 %) (Ministerio de Agricultura, Pesca y Alimentación, 2020; Instituto para a Conservação da Natureza e das Florestas, 2020; Cardil Forradellas et al., 2016; Fernandes et al., 2019; Büttner, 2014).

2.2. Sentinel-2 data

In this study, 11 Sentinel-2 tiles (44 images) were downloaded for Spain and Portugal regions, being all of them level 2A (atmospherically, radiometrically and geometrically corrected) (Büttner, 2014; Copernicus Open Access Hub, 2020; Kaufman and Sendra, 1988). The downloaded images are as close as possible to the fire without the presence of clouds (during October 22 to November 11 the study area was mostly covered by clouds). Table 1 shows a summary of all images used in this study (the days before and after the fire for each sensing date are shown in parentheses) and Table 2 shows the Sentinel-2 original bands with their respective central wavelengths (ESA, 2015).

Table 1
Sentinel-2 images downloaded tiles with their respective sensing dates (the days before and after the fire for each sensing date are shown in parentheses).

Country	Sentinel-2 Tiles	Sensing dates			
		Pre (less than 24 h (Galicia) and 30 days (Portugal) before first wildfire)	Post-1 (29 days (Galicia) and 26 days (Portugal) after last wildfire)	Post-2 (69 days (Galicia) and 66 days (Portugal) after last wildfire)	Post-3 (106 days (Galicia and Portugal) after last wildfire)
Spain	TNG	02/10/2017	14/11/2017	24/12/2017	30/01/2018
	TNH	02/10/2017	14/11/2017	24/12/2017	30/01/2018
Portugal	TNE	12/09/2017	11/11/2017	21/12/2017	30/01/2018
	TME	12/09/2017	11/11/2017	21/12/2017	30/01/2018
	TNF	12/09/2017	11/11/2017	21/12/2017	30/01/2018
	TMF	12/09/2017	11/11/2017	21/12/2017	30/01/2018
	SMD	12/09/2017	11/11/2017	21/12/2017	30/01/2018
	SND	12/09/2017	11/11/2017	21/12/2017	30/01/2018
	SPD	12/09/2017	11/11/2017	21/12/2017	30/01/2018
	TPE	12/09/2017	11/11/2017	21/12/2017	30/01/2018
	TPF	12/09/2017	11/11/2017	21/12/2017	30/01/2018

2.3. EFFIS data

The European Forest Fire Information Service (EFFIS) algorithm was initially implemented in 2003 to map burned areas during the fire season (Miller and Thode, 2007; Picotte and Robertson, 2011; San-Miguel-Ayanz et al., 2012). The Rapid Damage Assessment (RDA) module of EFFIS, maps burned areas during the fire season by analyzing daily images of Moderate Resolution Imaging Spectroradiometer (MODIS), aboard TERRA and AQUA satellites, using the red and near infrared bands (250 m), the short wave infrared bands (500 m) and the active fire product of MODIS (1 km) (Giglio et al., 2003; Roy et al., 2005, 2007). EFFIS provides the daily update of the perimeters of burnt areas in Europe for fires of about 30 ha or larger, twice every day. Small burnt or un-burnt areas below the spatial resolution of the MODIS imagery are not mapped; these may include small unburned islands inside the burnt area (Roy et al., 2005, 2007; Neumann et al., 2007). The omission of these small burned and unburned areas will mean an increase in omission and commission errors, respectively, impacting in total burned area. Furthermore, fire severity is estimated using the differenced Normalized Burn Ratio (dNBR) algorithm (250 m) and verified through correlation with field-estimated fire effects (Lutes et al., 2006; Twele, 2004). In this study, EFFIS fire severity is used for Sentinel-2 dNBR validation. Clouds of MODIS data are removing using a cloud mask based on the MOD35 product at 1 km resolution (Ackerman, 1997).

For this study, the dates of the burned areas obtained by EFFIS range from the same day that the fire was extinguished to 10 days later (depending on fire). For burn severity, dates are not available.

2.4. Reference data

For Spanish burned areas, MAPAMA service uses GPS data combined with burnt area cartography obtained by fire experts, meanwhile, in Portugal, ICNF service uses a combination of GPS data, Landsat-8 satellite images (Barsi et al., 2014) and EFFIS information. The spatial resolution of MAPAMA and ICNF data is not available, except Landsat-8 (15–100 meters and EFFIS (250 m). In addition, ICNF data has been improved with the contribution of the EMS delineation map (ID: EMSR250), which use detects the presence of unburned islands within burned areas (Emergency Mapping Service (EMS, 2019). For Portugal forest fires, the EMS burned areas map is based in high spatial resolution remote sensing data as Sentinel-2 (10−20 meters), SPOT-6 (2–8 meters) and SPOT-7 (2–8 meters) satellite images (Emergency Mapping Service (EMS, 2019; Sedaghat and Ebadi, 2015; Toth and Jóźków, 2016). Moreover, for burn severity levels case, EFFIS data is used as a reference

Table 2
Sentinel-2 bands with their respective central wavelengths and spatial resolutions.

Number of band	Name	Central wavelength (nm)	Spatial resolution (m)
1	Coastal aerosol	443	60
2	Blue	490	10
3	Green	560	10
4	Red	665	10
5	Red-edge 1	705	20
6	Red-edge 2	740	20
7	Red-edge 3	783	20
8	NIR	842	10
8a	NIR narrow	865	20
9	Water vapour	945	60
10	Cirrus	1375	60
11	SWIR 1	1610	20
12	SWIR 2	2190	20

because it is the only source of information that provides burn severity results on a periodic basis and for the whole of Europe (European Forest Fire Information System (EFFIS, 2020). This information was acquired by request using the website steps.

2.5. Preprocessing

Firstly, all Sentinel-2 bands used for the calculation of spectral indices have been resampled (from 20 to 10 m) and clipped using SNAP software (Novák et al., 2018). Despite having checked for the presence of clouds prior to downloading images, it ensures the removal of pixels classified as clouds using the Scene Classification Image (SCL) mask (Copernicus Open Access Hub, 2020; Kaufman and Sendra, 1988). To find out which bands best discriminate between unburned and burned areas, Fig. 2 shows a comparison of all Sentinel-2 bands reflectances inside burned areas, except bands 1, 9 and 10 because they are related to the study of the atmosphere and not to the land surface (Table 2), for the four study dates (Table 1).

The comparison of Sentinel-2 spectral curves in all study dates (Fig. 2) indicates some conclusions. Firstly, there is a decrease in reflectance in the Green and NIR spectrum regions between the Pre and Post fire images (disappearance of vegetation cover) and an increase in reflectance from 2200 nm (SWIR 2 band) over time due to the decrease in water absorption. Second, in the case of post-fire images, reflectance increases in all regions (especially in the SWIR zone) over time. In addition, there is a similarity between healthy vegetation areas and the pre-fire image, and between bare soil areas and post-fire images (with the passing of time, the burned trees fall and, for this reason, the similarity with ground increases).

It is therefore concluded that the appropriate index for discriminating between burned and unburned areas is that which contains information in the NIR and SWIR spectrum regions. This is the case of the Normalized Burn Ratio (NBR) and the differenced NBR (dNBR), which is the index chosen, are obtained (Eq. 1 and Eq. 2) (Lutes et al., 2006; Mallinis et al., 2018; Amos et al., 2019; Huang et al., 2016; Key and Benson, 2005).

$$NBR = \frac{(NIR - SWIR)}{(NIR + SWIR)} \tag{1}$$

$$dNBR = NBR_{PRE-FIRE} - NBR_{POST-FIRE} \tag{2}$$

The dNBR index is very useful to determine burn surfaces and burn severity levels. It could be classified according to the classification proposed by the United States Geological Survey (USGS) but, in this study, the classification used is the proposed by EFFIS (Table3) (Twele, 2004; Key and Benson, 2005; U.S. Geological Survey, 2016) because the results obtained will be compared with EFFIS results.

Burned area pixels values are all those higher than or equal to 0.1 (low severity or higher based on Table 3 values). As the aim of this study is to analyze large forest fires, all forest fires below 500 ha are eliminated

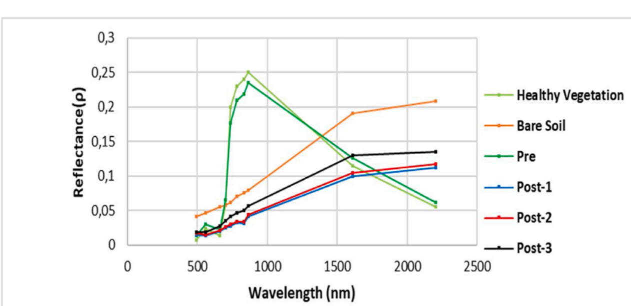

Fig. 2. Comparison of all Sentinel-2 bands reflectances inside burned areas, except bands 1, 9 and 10, for the four study dates (Pre, Post-1, Post-2 and Post-3).

Table 3
Differenced Normalized Burn Ratio (dNBR) thresholds proposed by the European Forest Fire Information Service (EFFIS).

EFFIS thresholds	Severity Level
dNBR < 0.100	Unburned / Very Low
0.100 ≤ dNBR ≤ 0.255	Low
0.256 ≤ dNBR ≤ 0.419	Moderate
0.420 ≤ dNBR ≤ 0.660	High
dNBR > 0.660	Very High

using the QGIS 2.18 raster to polygon tool. This process involves that EFFIS omission errors are minimized more than EFFIS commission errors because the capability of missing a small fire is reduced.

In addition, in the study area, the water bodies are removed in order to avoid noise pixels in dNBR algorithm image. In this sense, the Normalized Difference Water Index (NDWI) is proposed (Eq. 3) (McFeeters, 1996).

$$NDWI = \frac{(Green - NIR)}{(Green + NIR)} \tag{3}$$

Fig. 3, shows an example of the different dNBR images obtained in Galicia and Portugal using Sentinel-2 (for Post-1 sensing date) and EFFIS data.

2.6. Fire perimeter delimitaion

The fire perimeter delimitation result is based on the comparison between the spectral index dNBR (using Sentinel-2 post fire images or EFFIS) and the reference perimeters (GPS, EMS and ICNF perimeters) (Amos et al., 2019; Filipponi, 2019; Brown et al., 2018; Teodoro and Amaral, 2019; Key and Benson, 1999). First of all, the spectral indices (SPI) are reclassified using a threshold of 0.1 (low severity or higher based on Table 3 values) where burned areas are pixels which value is 1 and unburned areas are pixels which value is 0. s, reference perimeters (RP) are also reclassified where burned areas are pixels which value is 2 and no burned areas are pixels which value is 0. Finally, both perimeters are summed and interpreted following the classification in Table 4.

To analyze the accuracy of pixel values (Table 4), the following algorithms are used:

$$Coincidence\ Area\ (COI) = \frac{COIP}{COIP + OP} * 100 \tag{4}$$

$$Omission\ Area\ (OM) = \frac{OP}{COIP + OP} * 100 \tag{5}$$

$$Commission\ Area\ (COM) = \frac{CP}{COIP + CP} * 100 \tag{6}$$

The result of Eqs. 4,5 and 6 are expressed in percentages. The coincidence area (COI) measures the SPI capacity to correctly delineation the burned area compared to the RP. The omission area (OM) measures the pixels, which SPI detects as fire, but the RP detects as no fire. Otherwise, the commission area (COM) measures the pixels, which SPI detects as no fire, but the RP detects as fire (Amos et al., 2013; Huesca et al., 2013; Hermosilla et al., 2017).

2.7. Burn severity levels

The burn severity levels result is based on the spectral index dNBR (using Sentinel-2 post fire images) classified using the EFFIS thresholds (Table 3). To assess the separability of the Sentinel-2 burn severity levels, the Separability Index (SI) is applied in this study (Eq. 7) (Kaufman and Remer, 1994; Lasaponara, 2006; Pereira, 1999).

$$SI = \frac{|\mu_1 + \mu_2|}{\sigma_1 - \sigma_2} \tag{7}$$

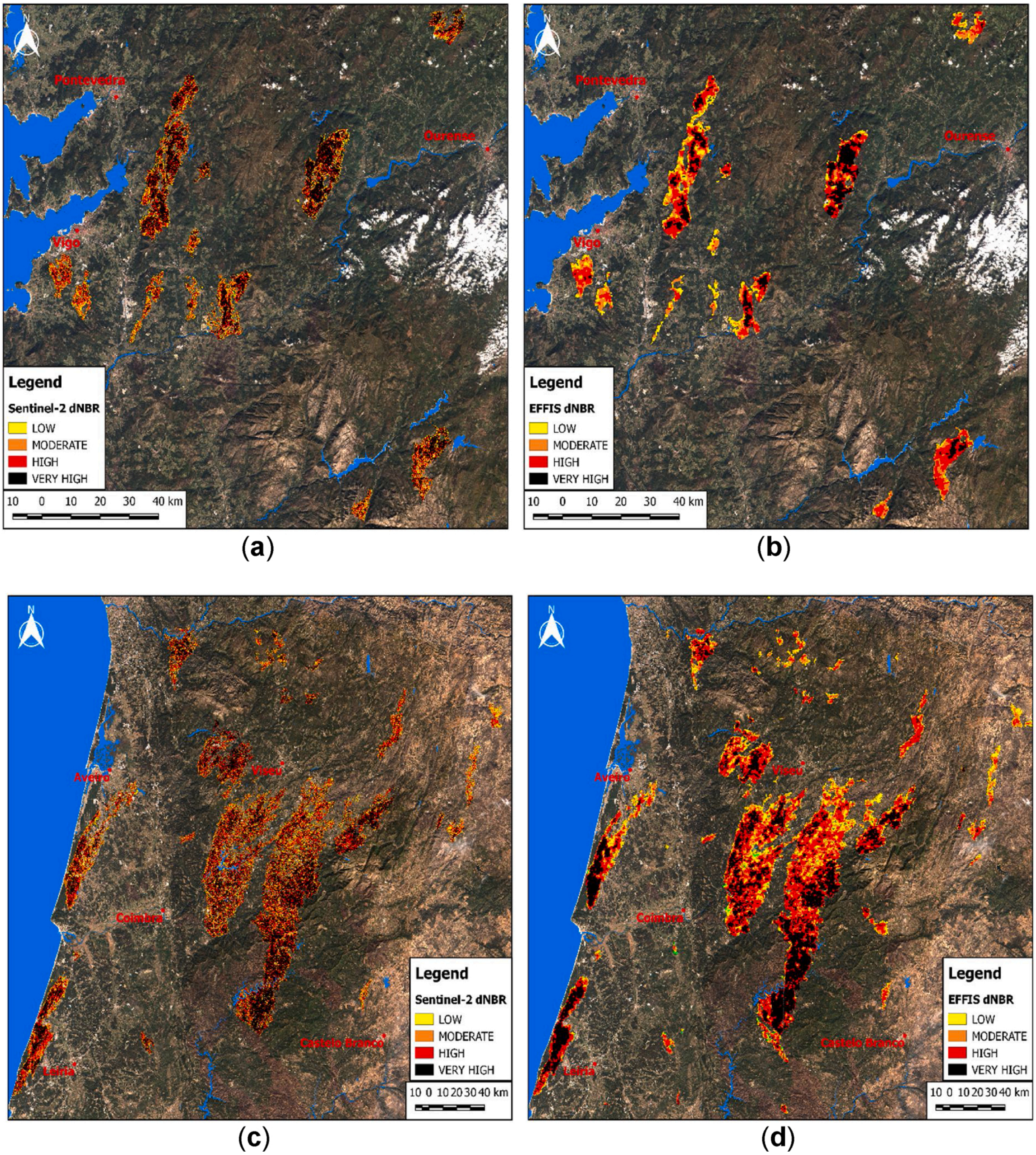

Fig. 3. (**a**) Sentinel-2 dNBR image using Post-1 images in Galicia wildfires; (**b**) EFFIS dNBR image in Galicia wildfires; (**c**) Sentinel-2 dNBR image using Post-1 images in Portugal wildfires; (**d**) EFFIS dNBR image in Portugal wildfires. Water areas are masked (blue color). (For interpretation of the references to colour in the Figure, the reader is referred to the web version of this article).

Table 4
Interpretation of the fire perimeter delimitation results where SPI is Spectral Indices and RP is Reference Perimeters.

Pixel Values	Classes
SPI + RP = 0	No Fire Pixels (NF)
SPI + RP = 1	Commission Pixels (CP)
SPI + RP = 2	Omission Pixels (OP)
SPI + RP = 3	Coincidence Pixels (COIP)

where, on the one hand, $\mu 1$ and $\mu 2$ are the mean values of Sentinel-2 dNBR index, for random points (obtained using the QGIS 2.18 random points tool) within EFFIS and Sentinel-2 coincidence perimeter, at each EFFIS burn severity degree (Table 3). The random points obtained are based on a burned surface criteria (larger burned area, more points inside). On the other hand, $\sigma 1$ and $\sigma 2$ are the standard deviations of Sentinel-2 dNBR index for each point. Values of SI higher than 1 show that the index allows for a good separation between Sentinel-2 burn severity levels (Lasaponara, 2006). Fig. 4 shows the spatial distribution of these points in Galicia and Portugal fires and Table 5 summarizes the number of validation points for each EFFIS burn severity level.

The 83 points classified as unburned / very low severity are due to

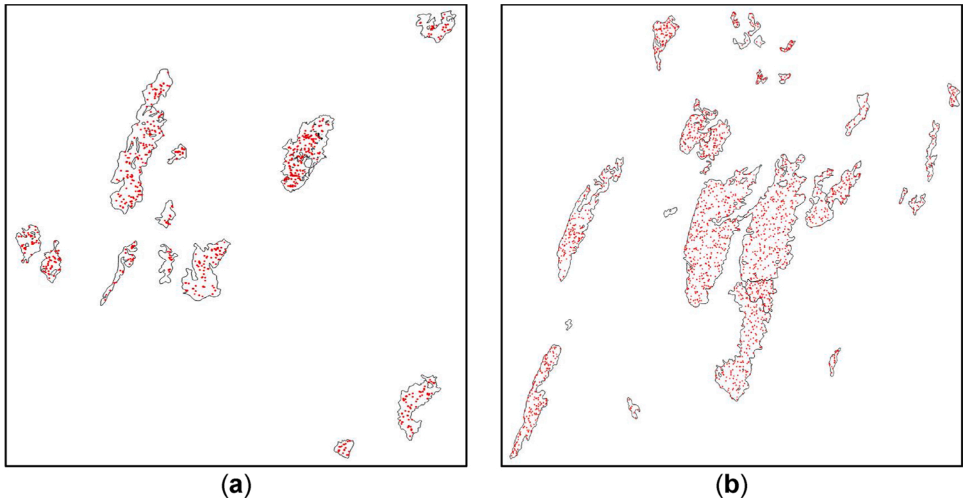

Fig. 4. (**a**) Spatial distribution of random points in Galicia wildfires; (**b**) Spatial distribution of random points in Portugal wildfires. Reference fire perimeters (black colour) for Spain (MAPAMA) and Portugal (ICNF, EMS) fires are displayed.

Table 5
Number of validation points for each EFFIS burn severity degree.

Burn severity levels	Number of points
Unburned / Very Low	83
Low	250
Moderate	465
High	906
Very High	780
Total	1500

the different ways that EFFIS uses to obtain burned areas and burn severity. First, burned areas are obtained by a combination of unsupervised and supervised classification. After this, burn severity is obtained by dNBR algorithm. Therefore, when the severity is obtained, areas where the severity is very low or even unburned could appear.

In addition to SI, in general, previous studies use other methodologies for burn severity assessment as the confusion matrix (Muñoz, 2016; Congalton, 2001) which allows demonstrate the correlation between Sentinel-2 and EFFIS results. The confusion matrix provides three different results of accuracy: a) omission error (error related to the percentage of EFFIS data properly classified for each burn severity degree); b) commission error (error related to the percentage of Sentinel-2 dNBR data properly classified for burn severity degree; c) Kappa statistic (displays the agreement percentage of a classification, after removing the portion due to randomness). Their values range from zero to one, being the value 1 the case of total agreement (Congalton and Green, 2002).

3. Results

Table 6 shows the fire perimeter results for each index (the EFFIS dNBR and the Sentinel-2 dNBR index using different post-fire sensing dates displayed in Table 1) where the highest values of Coincidence Area (COI) and the lowest values of Omission Area (OM) and Commission Area (COM) determine the best index to differentiate between burned and unburned areas. The results are expressed in ha and percentages.

The assessment of the fire perimeter delimitation was carried out using Eqs. 4,5 and 6 (Amos et al., 2019; Petropoulos et al., 2011). The results, displayed in Table 6, show the dNBR Post-1 index as the best choice (taking into account the COI, OM and COM values) to differentiate between burned an unburned areas (245,632 ha (91 %), 25,192 ha (9%) and 39,427 ha (14 %)). Nevertheless, this index results are very similar to the dNBR Post-2 indices (a 5% of difference as maximum). In addition, the EFFIS dNBR index is the most similar to dNBR Post-1 index in COI and OM variables but, in COM sense, the error is an 11 % higher (75,737 ha (24 %)).

Besides in the case of fire perimeter results, Table 7 shows the burn severity levels results for each index where the highest values of Separability Index (SI) determine the best index to differentiate between the different burn severity levels.

The dNBR Post-3 image shows the highest SI between Unburned / Very Low - Low and Moderate – High (1.20 and 1.29, respectively), and the dNBR Post-1 image shows the highest SI between Low – Moderate and High – Very High (1.13 and 1.23, respectively). However, the dNBR Post-2 image hows the lowest SI between Unburned / Very Low - Low and High – Very High (1.02 and 1.11, respectively), the dNBR Post-3 image shows the lowest SI between Low – Moderate (1.04) and the dNBR Post-1 image shows the lowest SI between Moderate – High (1.21). In Global sense, both dNBR Post-1 image and dNBR Post-3 image

Table 6
Fire perimeter results based on Coincidence Area (COI), Omission Area (OM) and Commission Area (COM), and using the EFFIS and the Sentinel-2 (for each post-fire sensing date displayed in Table 1) differenced Normalized Burn Ratio (dNBR) index for Galicia and Portugal wildfires. The results are expressed in ha and percentages (in parentheses).

	Remote sensing indices			
	Post-1	Post-2	Post-3	EFFIS
COI	245,632 ha (91 %)	239,000 ha(89 %)	230,855 ha(86 %)	243,419 ha(90 %)
OM	25,192 ha(9%)	30,927 ha(11 %)	39,071 ha(14 %)	26,507 ha (10 %)
COM	39,427 ha(14 %)	39,255 ha(14 %)	37,211 ha(14 %)	75,737 ha (24 %)

Table 7
Burn severity levels results based on the Separability Index (SI), and using the random points displayed in Fig. 4 and Table 5, the EFFIS and the Sentinel-2 (for each post-fire sensing date displayed in Table 1) differenced Normalized Burn Ratio (dNBR) index for Galicia and Portugal wildfires.

	Remote sensing indices		
	Post-1	Post-2	Post-3
Unburned / Very Low - Low	1.06	1.02	1.20
Low – Moderate	1.13	1.11	1.04
Moderate – High	1.21	1.23	1.29
High – Very High	1.23	1.11	1.12
Global	1.16	1.12	1.16

Table 8
Omission (OE) and Commission errors (CE) based on the matrix confusion, and using the random points displayed in Fig. 4 and Table 5, the EFFIS and the Sentinel-2 (for each post-fire sensing date displayed in Table 1) differenced Normalized Burn Ratio (dNBR) index for Galicia and Portugal wildfires.

	Remote sensing indices					
	Post-1		Post-2		Post-3	
	OE (%)	CE (%)	OE (%)	CE (%)	OE (%)	CE (%)
Unburned / Very Low	8	17	26	23	21	8
Low	30	31	27	32	42	37
Moderate	37	30	39	32	31	35
High	20	26	24	22	24	27
Very High	10	7	8	11	13	12
Global	21	22	25	24	26	24

(show the highest results (1.16) but dNBR Post-2 image shows the lowest result (1.12).

In addition to SI results, Table 8 shows the omission (OE) and commission (CE) errors obtained for each burn severity degree and Sentinel-2 index and Table 9 shows the Kappa statistic (k) for each Sentinel-2 dNBR index.

The dNBR Post-1 image provides the highest results in OE (21 %), CE (22 %) and k (0.73), but with similar values to dNBR Post-2 image and Post-3 image (Table 8 and 9). The burn severity degree with the highest result is very high, which OE range is between 8 and 13 % and CE range is between 7 and 12 %. On the contrary, the burn severity degree with the lowest result is moderate, which OE range is between 31 and 39 % and CE range is between 30 and 35 %.

4. Discussion

The European Forest Fire Information Service (EFFIS) provides a large amount of global fire perimeters, burned areas and burn severity levels but, in some cases, it has some limitations which can be improved (San-Miguel-Ayanz et al., 2012). Until now, most of the work related to remote sensing and forest fires was carried out using images time series with low spatial resolution (as in the case of the MODIS sensor). Other studies also use a group of spectral indices and only two images (pre and post-fire) with medium and high spatial resolution (Sentinel-2 and SPOT images, among others) (Navarro et al., 2017). For this reason, this work incorporates the innovation of using Sentinel-2 with more than one post fire image applied in Galicia and Portugal wildfire events but due to the presence of clouds, the first downloaded images are one month after the fires were extinguished (11–14 of November 2017).

The comparison of Sentinel-2 spectral curves (in all study dates) shows a high correlation between Near Infrared (NIR) and Short Wave Infrared (SWIR) to discriminate between healthy vegetation and burned areas. For this reason, this study uses the differenced Normalized Burn Ratio (dNBR) which contains information in the NIR and SWIR spectrum regions and it is commonly used in burned areas detection (Key and Benson, 2005).

The EFFIS fire perimeter data is provided with a high temporal frequency (two times per day against five days in Sentinel-2 sense) but with low spatial resolution (250 m against 10 or 20 m in Sentinel-2 sense). For this reason, using the Sentinel-2 dNBR, slightly more accurate results are obtained (especially in the case of commission errors where Sentinel-2 commits 35,000 Ha (10 %) less than EFFIS, in all cases) comparing them with the reference data (GPS perimeters and high resolution images). In addition, it should be noted that the Sentinel-2 errors observed may be lower. Firstly, some omission errors would be due to internal islands (unburned areas within the fire) that the reference image does not detect. Secondly, some of the commission errors would be due to areas that are difficult to access for GPS data collection. It is also important to highlight that the results are better when a post fire image is used as close as possible to the fire extinction date (over time, climate factors such as rain can disturb results). This study results differ from previous studies that use EFFIS data or high spatial resolution images as reference data. In this work, the best COI and COM values are lower than the study carried out by Donezar-Hoyos et al., 2017 (2335 ha (99 %) of COI and 995 ha (30 %) of COM), using Sentinel-2 images and Pléiades image (0.5 m of spatial resolution) as reference data, but the Donezar-Hoyos et al., 2017 OM value is lower than the obtained in this study (24 ha (1%) of OM) (Bernard et al., 2012). In contrast, in Donezar-Hoyos et al., 2017 study, the burned area analyzed are less than in this study, therefore, the possibility of commit errors are less than in this study). Another example is the study realized by Boschetti et al., 2008, which uses the MODIS fire product (MCD45) and the EFFIS data as reference data (Boschetti et al., 2009). In this case, the fire perimeter results are very similar but lower than obtained in this study (242,900 ha (89 %) of COI, 49,758 ha (17 %) of COM and 29,263 (11 %) of OM) (Arellano, et al., 2017). The use of a low spatial resolution data satellite data as MCD45 (500 m) in Boschetti et al., 2008 study has the limitation of small burned areas detection (less accuracy in COI, OM and COM results).

Finally, the assessment of the burn severity levels was carried out using the Separability Index (SI) showed in Eq. 7 (Kaufman and Remer, 1994; Lasaponara, 2006; Pereira, 1999) and the confusion matrix results showed in Table 8 and 9. Table 7 shows a good discrimination between burn severity levels based on all the SI results are higher than one (Lasaponara, 2006). The dNBR Post-1 image and the dNBR Post-3 image provide the best results (SI equal to 1.16), but the dNBR Post-2 image provides a similar result (SI equal to 1.12). In addition, confusion matrix global results obtained in this study (OE between 21 and 26 %, CE between 22 and 24 % and Kappa (k) between 0.69 and 0.73) are different than obtained by Arellano et al., 2017 using the CBI field measurements as reference data (OE between 20 and 21 %, CE between 20 and 29 % and k equal to 0.56) (Boschetti, et al., 2008). The OE and CE results obtained in this study are lower than the OE and CE obtained by Arellano et al., 2017 but in the case of Kappa, it is the opposite. The reason of this is that, in Arellano et al., 2017 study, are used three burn severity levels (low, moderate and high) and the Kappa statistic functions better when it has more classes (Muñoz, 2016; Congalton, 2001; Congalton and Green, 2002). In addition, it is important to taking into account that Kappa statistic has some limitations related to accuracy as randomness and redundant results when it measures overall accuracy (Rozario et al., 2018; Pontius and Millones, 2011; Ye et al., 2018).

Table 9
Kappa statistic (k) based on the matrix confusion, and using the random points displayed in Fig. 4 and Table 5, the EFFIS and the Sentinel-2 (for each post-fire sensing date displayed in Table 1) differenced Normalized Burn Ratio (dNBR) index for Galicia and Portugal wildfires.

	Remote sensing indices		
	Post-1	Post-2	Post-3
Kappa (k)	0.73	0.72	0.69

5. Conclusions

The present study aimed a methodology to estimate the burned areas extent and the burn severity levels using Sentinel-2 images to the fires occurred in October 2017 in Spain and Portugal. The results obtained showed that Sentinel-2 dNBR provides a useful alternative to EFFIS data in wildfire works.

On one hand, this study shows that, for Galicia and Portugal areas, the images several months after the fire date offer satisfactory results (coincidences higher than 230,000 ha (85 %) and errors less than 40,000 ha (15 %) in all cases). Hence, in fire perimeter delimitation sense, this article concludes that Sentinel-2 dNBR is a good alternative to EFFIS fire perimeter, especially when there is a need to detect details inside the fire (results with higher spatial resolution work slightly better than results with higher temporal resolution).

On the other hand, the EFFIS burn severity service is the unique global information provided openly now. However, it is only provided as soon as they have the best images available (in some cases, two times per year). The statistical analyses carried out in this study (Separability index (SI) and confusion matrix) show a good correlation with all EFFIS burn severity levels. SI analysis shows a good discrimination between burn severity levels (all the values are higher than 1) in all post fire images, but in matrix confusion sense, as in the case of fire perimeter delimitation, the results are slightly better when a post fire image is used as close as possible to the fire extinction date. Finally, the Kappa statistic shows a substantial agreement between EFFIS and Sentinel-2 burn severity levels (both use the dNBR index). Hence, in burn severity levels sense, this article concludes that Sentinel-2 dNBR is a good alternative to EFFIS burn severity levels, especially when there is a need to obtain a fire severity map with high spatial resolution and temporal frequency (in 2019, no EFFIS burn severity data are available).

In conclusion, this article demonstrates the high accuracy of Sentinel-2 dNBR index to fire perimeter delimitation and burn severity levels assessment as an alternative to EFFIS data. In future works the use of a larger and more heterogeneous burned areas database and the integration of new spectral indices related to wildfire could be necessary.

Funding

This research was funded by the research project EPyRIS, which is part of the Interreg SUDOE program of the European Union; project number SOE2/P5/E0811.

CRediT authorship contribution statement

Rafael Llorens: Formal analysis, Software, Visualization, Writing - original draft, Writing - review & editing. **José Antonio Sobrino:** Conceptualization, Funding acquisition, Investigation, Methodology, Project administration, Resources, Supervision, Writing - original draft, Writing - review & editing. **Cristina Fernández:** Conceptualization, Funding acquisition, Investigation, Methodology, Supervision, Writing - review & editing. **José M. Fernández-Alonso:** Investigation, Writing - review & editing. **José Antonio Vega:** Investigation, Methodology, Supervision, Writing - review & editing.

Declaration of Competing Interest

The authors declare that they have no known competing financial interests or personal relationships that could have appeared to influence the work reported in this paper.

Acknowledgments

The authors thank the editor-in-chief, the anonymous associate editor, and the reviewers for their systematic review and valuable comments.

References

Ackerman, S.A., 1997. Remote sensing aerosols using satellite infrared observations. J. Geophys. Res. Atmos. 102 (D14), 17069–17079.

Amos, C., Petropoulos, G.P., Ferentinos, K.P., 2019. Determining the use of Sentinel-2A MSI for wildfire burning & severity detection. Int. J. Remote Sens. 40 (3), 905–930.

Arellano, S., Vega, J.A., Rodríguez y Silva, F., Fernández, C., Vega-Nieva, D., Álvarez-González, J.G., Ruiz-González, A.D., 2017. Validación de los índices de teledetección dNBR y RdNBR para determinar la severidad del fuego en el incendio forestal de Oia-O Rosal (Pontevedra) en 2013. Revista de Teledetección (49), 49–61.

Barsi, J., Lee, K., Kvaran, G., Markham, B., Pedelty, J., 2014. The spectral response of the Landsat-8 operational land imager. Remote Sens. 6 (10), 10232–10251.

Bergamaschi, P., Hein, R., Brenninkmeijer, C.A., Crutzen, P.J., 2000. Inverse modeling of the global CO cycle: 2. Inversion of 13C/12C and 18O/16O isotope ratios. J. Geophys. Res. Atmos. 105 (D2), 1929–1945.

Bernard, M., Decluseau, D., Gabet, L., Nonin, P., 2012. 3D capabilities of Pleiades satellite. Int. Arch. Photogramm. Remote Sens. Spatial Inf. Sci 39, B3.

Boschetti, L., Roy, D., Barbosa, P., Boca, R., Justice, C., 2008. A MODIS assessment of the summer 2007 extent burned in Greece. Int. J. Remote Sens. 29 (8), 2433–2436.

Boschetti, L., Roy, D., Hoffmann, A.A., 2009. MODIS collection 5 burned area Product-MCD45. User's Guide, Ver 2.

Brown, A.R., Petropoulos, G.P., Ferentinos, K.P., 2018. Appraisal of the Sentinel-1 & 2 use in a large-scale wildfire assessment: a case study from Portugal's fires of 2017. Appl. Geogr. 100, 78–89.

Büttner, G., 2014. CORINE land cover and land cover change products. In Land Use and Land Cover Mapping in Europe. Springer, Dordrecht, pp. 55–74.

Cardil Forradellas, A., Molina Terrén, D., Oliveres, J., Castellnou, M., 2016. Fire effects in Pinus uncinata Ram plantations. For. Syst. 25 (1), eSC06. https://doi.org/10.5424/fs/2016251-08919.

Chen, X., Vogelmann, J.E., Rollins, M., Ohlen, D., Key, C.H., Yang, L., Shi, H., 2011. Detecting post-fire burn severity and vegetation recovery using multitemporal remote sensing spectral indices and field-collected composite burn index data in a ponderosa pine forest. Int. J. Remote Sens. 32 (23), 7905–7927.

Chuvieco, E., 2009. Global impacts of fire. Earth Observation of Wildland Fires in Mediterranean Ecosystems. Springer, Berlin, Heidelberg, pp. 1–10.

Chuvieco, E., Riaño, D., Van Wagtendok, J., Morsdof, F., 2003. Fuel loads and fuel type mapping. In Wildland Fire Danger Estimation and Mapping: the Role of Remote Sensing Data, pp. 119–142.

Congalton, R.G., 2001. Accuracy assessment and validation of remotely sensed and other spatial information. Int. J. Wildland Fire 10 (4), 321–328.

Congalton, R.G., Green, K., 2002. Assessing the Accuracy of Remotely Sensed Data: Principles and Practices. CRC press.

Copernicus Open Access Hub. Available online: https://scihub.copernicus.eu/dhus/#/home (accessed on 20 January 2019).

Donezar-Hoyos, U., Larrañaga Urien, A., Tamés-Noriega, A., Sánchez-Gil, C., Albizua-Huarte, L., Ciriza-Labiano, R., del Barrio-Arellano, F., 2017. Aplicación de imágenes Sentinel-1 y Sentinel-2 en la detección y delineación de información de crisis de desastres naturales en el marco de los servicios Copernicus EMS. Revista de Teledetección 50, 49–57.

Emergency Mapping Service (EMS). Available online: https://emergency.copernicus.eu/mapping/list-of-components/EMSR250 (accesed on 18 January 2019).

ESA, 2015. Sentinel-2 User Handbook. European Spatial Agency, p. 64. ESA Standard Document.

Escuin, S., Navarro, R., Fernandez, P., 2008. Fire severity assessment by using NBR (normalized burn ratio) and NDVI (Normalized Difference Vegetation Index) derived from LANDSAT TM/ETM images. Int. J. Remote Sens. 29 (4), 1053–1073.

European Forest Fire Information System (EFFIS). Available online: http://effis.jrc.ec.europa.eu/applications/data-request-form/ (accessed on 18 January 2019).

Fernandes, P.M., Guiomar, N., Rossa, C.G., 2019. Analysing eucalypt expansion in Portugal as a fire-regime modifier. Sci. Total Environ. 666, 79–88.

Fernández-Manso, A., Fernández-Manso, O., Quintano, C., 2016. SENTINEL-2A red-edge spectral indices suitability for discriminating burn severity. Int. J. Appl. Earth Obs. Geoinf. 50, 170–175.

Filipponi, F., 2019. Exploitation of Sentinel-2 time series to map burned areas at the national level: a case study on the 2017 Italy Wildfires. Remote Sensing 11 (6), 622.

Giglio, L., Descloitres, J., Justice, C.O., Kaufman, Y.J., 2003. An enhanced contextual fire detection algorithm for MODIS. Remote Sens. Environ. 87 (2–3), 273–282.

Hermosilla, T., Wulder, M.A., White, J.C., Coops, N.C., Hobart, G.W., 2017. Updating Landsat time series of surface-reflectance composites and forest change products with new observations. Int. J. Appl. Earth Obs. Geoinf. 63, 104–111.

Huang, H., Roy, D., Boschetti, L., Zhang, H., Yan, L., Kumar, S., et al., 2016. Separability analysis of Sentinel-2A multi-spectral instrument (MSI) data for burned area discrimination. Remote Sens. 8 (10), 873.

Huesca, M., de Miguel, S.M., Alonso, F.G., Garcia, C.V., 2013. An intercomparison of satellite burned area maps derived from MODIS, MERIS, SPOT-VEGETATION and ARST images. An application to the August 2006 Galicia (Spain) forest fires. For. Syst. 22 (2), 222–231.

Instituto para a Conservação da Natureza e das Florestas. Available online: http://www2.icnf.pt/portal/florestas/dfci/inc/mapas (accessed on 18 January 2019).

Kaufman, Y.J., Remer, L.A., 1994. Detection of forests using mid-IR reflectance: an application for aerosol studies. IEEE Trans. Geosci. Remote. Sens. 32 (3), 672–683.

Kaufman, Y.J., Sendra, C., 1988. Algorithm for automatic atmospheric corrections to visible and near-IR satellite imagery. Int. J. Remote Sens. 9 (8), 1357–1381.

Key, C.H., Benson, N.C., 1999. Measuring and remote sensing of burn severity. In: In Proceedings Joint Fire Science Conference and WorkshopUniversity of Idaho and International Association of Wildland Fire Moscow, ID, 2, p. 284. June.

Key, C.H., Benson, N.C., 2005. Landscape assessment: remote sensing of severity, the normalized burn ratio and ground measure of severity, the composite burn index. FIREMON: Fire Effects Monitoring and Inventory System Ogden. Utah: USDA Forest Service, Rocky Mountain Res. Station.

Lasaponara, R., 2006. Estimating spectral separability of satellite derived parameters for burned areas mapping in the Calabria region by using SPOT-Vegetation data. Ecol. Modell. 196 (1–2), 265–270.

Lindner, M., Maroschek, M., Netherer, S., Kremer, A., Barbati, A., Garcia-Gonzalo, J., et al., 2010. Climate change impacts, adaptive capacity, and vulnerability of European forest ecosystems. For. Ecol. Manage. 259 (4), 698–709. https://doi.org/10.1016/j.foreco.2009.09.023.

Lutes, D.C., Keane, R.E., Caratti, J.F., Key, C.H., Benson, N.C., Sutherland, S., Gangi, L.J., 2006. FireMON: fire effects monitoring and inventory system. Gen. Tech. Rep. RMRS-GTR-164. US Department of Agriculture, Forest Service, Rocky Mountain Research Station, Fort Collins, CO, p. 164, 1 CD.

Mallinis, G., Mitsopoulos, I., Chrysafi, I., 2018. Evaluating and comparing Sentinel 2A and Landsat-8 Operational Land Imager (OLI) spectral indices for estimating fire severity in a Mediterranean pine ecosystem of Greece. GIsci. Remote Sens. 55 (1), 1–18.

McFeeters, S.K., 1996. The use of the Normalized Diff ;erence Water Index (NDWI) in the delineation of open water features. Int. J. Remote Sens. 17, 1425–1432.

Miller, J.D., Thode, A.E., 2007. Quantifying burn severity in a heterogeneous landscape with a relative version of the delta normalized Burn Ratio (dNBR). Remote Sens. Environ. 109 (1), 66–80.

Ministerio de Agricultura, Pesca y Alimentación. Available online: https://www.mapa.gob.es/es/ (accessed on 18 January 2019).

Muñoz, J.M.S., 2016. Análisis de calidad cartográfica mediante el estudio de la matriz de confusión. Pensamiento Matemático 6 (2), 9–26.

Navarro, G., Caballero, I., Silva, G., Parra, P.C., Vázquez, Á., Caldeira, R., 2017. Evaluation of forest fire on Madeira Island using Sentinel-2A MSI imagery. Int. J. Appl. Earth Obs. Geoinf. 58, 97–106.

Neumann, K., Herold, M., Hartley, A., Schmullius, C., 2007. Comparative assessment of CORINE2000 and GLC2000: spatial analysis of land cover data for Europe. Int. J. Appl. Earth Obs. Geoinf. 9 (4), 425–437.

Novák, V., Křížová, K., Napitupulu, R.A.M., 2018. Influence of North sumatra maize (zea mays L.) Monocultuure on soil properties using free sentinel 2 imagery. In: In IOP Conference Series: Materials Science and Engineering. IOP Publishing (Vol. 420, No. 1, p. 012076) September.

Pereira, J.M., 1999. A comparative evaluation of NOAA/AVHRR vegetation indexes for burned surface detection and mapping. IEEE Trans. Geosci. Remote. Sens. 37 (1), 217–226.

Petropoulos, G.P., Kontoes, C., Keramitsoglou, I., 2011. Burnt area delineation from a uni-temporal perspective based on Landsat TM imagery classification using support vector machines. Int. J. Appl. Earth Obs. Geoinf. 13 (1), 70–80.

Picotte, J.J., Robertson, K.M., 2011. Validation of remote sensing of burn severity in south-eastern US ecosystems. Int. J. Wildland Fire 20 (3), 453–464.

Pontius Jr., R.G., Millones, M., 2011. Death to Kappa: birth of quantity disagreement and allocation disagreement for accuracy assessment. Int. J. Remote Sens. 32 (15), 4407–4429.

Roy, D.P., Jin, Y., Lewis, P.E., Justice, C.O., 2005. Prototyping a global algorithm for systematic fire-affected area mapping using MODIS time series data. Remote Sens. Environ. 97 (2), 137–162.

Roy, D.P., Boschetti, L., Justice, C.O., 2007. The global MODIS burned area product. Towards an Operational use of Remote Sensing in Forest Fire Management, p. 191.

Rozario, P., Madurapperuma, B., Wang, Y., 2018. Remote sensing approach to detect burn severity risk zones in Palo Verde National Park, Costa rica. Remote Sens. 10 (9), 1427.

San-Miguel-Ayanz, J., Schulte, E., Schmuck, G., Camia, A., Strobl, P., Liberta, G., et al., 2012. Comprehensive monitoring of wildfires in Europe: the European forest fire information system (EFFIS). In Approaches to Managing Disaster-Assessing Hazards, Emergencies and Disaster Impacts. IntechOpen.

Sedaghat, A., Ebadi, H., 2015. Distinctive order based self-similarity descriptor for multi-sensor remote sensing image matching. ISPRS J. Photogramm. Remote. Sens. 108, 62–71.

Seiler, W., Crutzen, P.J., 1980. Estimates of gross and net fluxes of carbon between the biosphere and the atmosphere from biomass burning. Clim. Change 2 (3), 207–247.

Sobrino, J.A., Llorens, R., Fernández, C., Fernández-Alonso, J.M., Vega, J.A., 2019. Relationship between soil burn severity in forest fires measured in situ and through spectral indices of remote detection. Forests 10 (5) (19994907).

Sousa, W.P., 1984. The role of disturbance in natural communities. Annu. Rev. Ecol. Syst. 15 (1), 353–391.

Teodoro, A., Amaral, A., 2019. A statistical and spatial analysis of Portuguese forest fires in summer 2016 considering landsat 8 and sentinel 2A data. Environments 6 (3), 36.

Toth, C., Jóźków, G., 2016. Remote sensing platforms and sensors: a survey. ISPRS J. Photogramm. Remote. Sens. 115, 22–36.

Twele, A., 2004. Post-fire Vegetation Regeneration: the Case Study of the" Massif De L'Étoile" Fire. European Commission Joint Research Centre.

U.S. Geological Survey, 2016. Landsat—EarthObservationSatellites; Version 1.1; U.S. Geological Survey Fact Sheet 2015–3081. U.S. Geological Survey, Washingotn, DC, USA.

Van der Meer, F.D., Van der Werff, H.M.A., Van Ruitenbeek, F.J.A., 2014. Potential of ESA's Sentinel-2 for geological applications. Remote Sens. Environ. 148, 124–133.

Van der Werff, H., Van der Meer, F., 2015. Sentinel-2 for mapping iron absorption feature parameters. Remote sens. 7 (10), 12635–12653.

Vega, J.A., Fontúrbel, T., Fernández, C., Arellano, A., Díaz-Raviña, M., Carballas, T., Martín, A., González-Prieto, S., Merino, A., Benito, E., 2013. Acciones Urgentes Contra La Erosión En Áreas Forestales Quemadas: Guía Para Su Planificación En Galicia Santiago de Compostela.

Vélez, R., Salazar, M., Troenesgaard, J., Saigal, R., Wade, D. D., & Lundsford, J. (1990). Fire. Unasylva (English ed.), 41(162), 3-38.

Vilar, L., Camia, A., San-Miguel-Ayanz, J., Martín, M.P., 2016. Modeling temporal changes in human-caused wildfires in Mediterranean Europe based on land use-land cover interfaces. For. Ecol. Manage. 378, 68–78.

White, J.D., Ryan, K.C., Key, C.C., Running, S.W., 1996. Remote sensing of forest fire severity and vegetation recovery. Int. J. Wildland Fire 6 (3), 125–136.

Ye, S., Pontius Jr., R.G., Rakshit, R., 2018. A review of accuracy assessment for object-based image analysis: from per-pixel to per-polygon approaches. ISPRS J. Photogramm. Remote. Sens. 141, 137–147.